Materials Science and Engineering B 325 (2026) 119130

Contents lists available at ScienceDirect

Materials Science & Engineering B

journal homepage: www.elsevier.com/locate/mseb

Polarization switching in ferroelectric films triggered by charge injection/extraction at interfaces

Lucian Pintilie [a,*], Georgia Andra Boni [a], Cristina Florentina Chirila [a], Luminita Mirela Hrib [a], Lucian Trupina [a], Cristian Mihail Teodorescu [a], Athanasios Dimoulas [a,b]

[a] National Institute of Materials Physics, Atomistilor 405A, Magurele, Romania

[b] Institute of Nanoscience and Nanotechnology, National Center for Scientific Research DEMOKRITOS, Neapoleos 27 and Patriarchou Gigoriou Str., 15341 Athens, Attiki, Greece

ARTICLE INFO

Keywords:
Ferroelectric
Polarization
Depolarization field
Switching
Charge injection

ABSTRACT

A new mechanism is proposed for polarization switching in metal-ferroelectric-metal (MFM) structures. The switching is triggered by charge injection at electrode or grain interfaces under an external field, opposite to the initial direction of polarization. Such injection destabilizes the compensation of the polarization, and is favored by disappearance of Schottky barriers at interfaces, leading to a resistive like behavior. At the coercive voltage the depolarization field is no longer compensated and the polarization change orientation parallel to the applied field. After switching, the Schottky barriers are restored and the current start to decrease although the voltage continues to increase. This leads to a differential negative resistance until the barriers are totally restored, polarization saturated on the new direction and the depolarization field annihilated by the injected charges. In a perfect structure the switching takes place homogeneously, while the defects presence induces domains via local nucleation and fields. The model is supported by theory, showing that at switching the MFM structure has a resistive like behavior, and by experiments, showing that the voltage dependence of the current during switching is linear and that the phase change at switching, in PFM measurements performed on high quality epitaxial films, is abrupt. The analysis was performed on MFM structures based on different ferroelectric layers (e.g. Pb(*Zr*,*Ti*)O_3, $BaTiO_3$, $BiFeO_3$ or $(HfZr)O_2$), different metal electrodes and different structural qualities. It appears that polarization switching triggered by charge injection at interfaces is a mechanism that can be applied to all MFM structures based on oxide ferroelectrics.

1. Introduction

Ferroelectric materials are of great interest due to their potential use in a variety of applications spanning from non-volatile memories, to domestic burglar alarms [1,2]. They are used in combination with metal contacts forming metal-ferroelectric-metal (MFM) structures that normally behaves as capacitors. Constant miniaturization of devices involving ferroelectric perovskites has imposed passage from bulk ceramics or crystals to thin films. The advance in the deposition techniques allow now to obtain ferroelectric layers of epitaxial quality, or at least highly textured in the direction perpendicular to electrodes [3,4]. Although considered as insulators, it was found that in MFM structures the ferroelectric behaves more like a wide gap semiconductor, the entire structure having a large but finite resistance. This can be dominated by the high resistance of the depleted regions occurring at the electrode interfaces, that behaves like Schottky type contacts [5–7].

One specific property of ferroelectrics that it is widely exploited in applications, especially non-volatile memories, is the polarization switching. At macroscopic scale, this property is studied by performing hysteresis measurements, rendering a polarization-voltage (P—V) loop from which one can extract the remnant and saturation values of polarization, and the coercive field. At nanoscale, the switching can be studied using piezoelectric force microscopy (PFM). The models for polarization switching assumes formation of domains with opposite directions of polarization. At the coercive voltage, when the polarization is zero, it is assumed that there are equal volumes with polarization in opposite directions. The presence of domains at nanoscale was demonstrated using PFM, but also other techniques, such as transmission electron microscopy (TEM) [8–12]. Therefore, one cannot deny their presence. The question is, do the domains form in any circumstances or

* Corresponding author.
E-mail address: pintilie@infim.ro (L. Pintilie).

https://doi.org/10.1016/j.mseb.2025.119130
Received 22 October 2025; Received in revised form 2 December 2025; Accepted 14 December 2025
Available online 21 December 2025
0921-5107/© 2025 The Authors. Published by Elsevier B.V. This is an open access article under the CC BY-NC license (http://creativecommons.org/licenses/by-nc/4.0/).

their presence/formation is generated by structural defects carrying charges and inducing local electric fields that influence the polarization switching? The theory predicts that domains form to minimize the free energy in a ferroelectric slab, assumed to be a perfect insulator and in the absence of metallic electrodes, thus without any free charge to compensate the depolarization field. When metallic electrodes are present, it is assumed that the depolarization field is compensated by the free carriers from the electrodes and a single domain state can be stabilized. The switching in this case assumes the nucleation and growth of domains with polarization opposite to its initial orientation [13–15]. The nuclei form on charged defects distributed in the volume of the ferroelectric film or at electrode interfaces, but what happens in the case of a perfect single crystal layer, with perfect electrode interfaces? Do the domains form in this case and, if they form, are stable? How can be achieved the zero-polarization state when domains are not forming? Experimental evidences started to occur supporting the hypothesis that domains may not form during switching in nearly perfect epitaxial MFM structures [16–18].

Among the popular models to simulate a polarization or current hysteresis loop are those based on the classic thermodynamic Landau-Ginzburg-Devonshire theory coupled with the Landau-Khalatnikov Eq. [19–21]. Despite their apparent success, thermodynamic based models, as well other models based on domains kinetic, do not consider two critical aspects that can have a significant impact on the hysteresis measurements: how the microstructure affects the shape of the loop and the values extracted for polarization and coercive field; how the newly developed depolarization field just after the switching is compensated to stabilize the new direction of polarization. The reports in the literature showing different shapes of hysteresis loops, and different values for remnant polarization and coercive field, for the same material composition are so abundant that it is not worthy to mention them as references. Just one can look for two popular materials, $BaTiO_3$ (BTO) and Pb(Zr,Ti)O_3 (PZT, e.g. with Zr/Ti ratio of 20/80), and one can find very different results, depending on the structural quality [22–25]. fact raises suspicions of what input data one can use to model a certain hysteresis loop or another. The second aspect mentioned above is also very important and imply a redistribution of the charges involved in the compensation of the depolarization field associated to the initial orientation of polarization. When polarization switches, those charges, either from the ferroelectric or from the electrodes, have to move from one interface to the other to stabilize the new polarization orientation. If the ferroelectric is assumed insulating, then those charges have to move through the external wiring, making the hysteresis measurement dependent on the experimental set-up. In reality, the ferroelectrics have finite resistance, implying that compensation charges can move through the MFM structure also. Therefore, there is a current flowing through the circuit and the hysteresis loop is obtained by integrating exactly this current, with all its components (displacement, leakage, other transient currents), when an a.c. voltage is applied in the MFM structure. In the ideal case, the displacement current should dominate.

The present study focusses on a comprehensive analysis of the current hysteresis loop. Based on this analysis it hypothesized that during the switching the MFM structure has a resistive like behavior and that the polarization switching is triggered by charge injection at the electrode interfaces in the case of epitaxial layers. The model can be extended to polycrystalline films, with the amendment that the charge injection in this case takes place not only at electrode interfaces but also at grain boundaries. The model assumes, based on theoretical considerations that, at the beginning of the switching (electric field applied opposite to polarization direction previously set in the MFM structure), the Schottky like barriers at interfaces are reduced or even disappear, facilitating injection of charges of opposite sign compared to those involved in the compensation of the depolarization field associated with the initial orientation of polarization. At coercive voltage, the depolarization field is no longer compensated and the polarization change orientation parallel to the applied electric field. Immediately after the switching the Schottky like barriers start to build up again at interfaces, gradually reducing the current magnitude until the depolarization field associated to the new direction of polarization is totally compensated and the ferroelectric polarization is stabilized to saturation value. The proposed model does not involve formation of ferroelectric domains, the switching being homogeneous in any part of the ferroelectric films that behaves as a single crystal. Domain forms however due to structural defects or other inhomogeneities generating local electric fields that hinder homogeneous switching. The model is supported by few experimental findings such as almost perfect rectangular P—V loops in the case of high quality epitaxial ferroelectric films, as well sharp switching in PFM when the voltage applied on the tip during scanning is gradually increased from maximum negative to maximum positive values. Based on the fact that the current hysteresis loop shows similar features for MFM structures of different ferroelectric materials (Pb(Zr,Ti)O_3, $BaTiO_3$, $BiFeO_3$ or (HfZr)O_2), with different electrodes and different structural qualities one can conclude that the proposed model is rather universal, at least for oxide type ferroelectrics. This model does not necessarily contradict the present models, but can explain the differences observed in hysteresis measurements performed on samples of the same material but of different structural qualities and different electrodes.

2. Preliminary considerations

2.1. Theory-equivalent circuit

The hysteresis measurement is, in principle, an a.c. measurement since on the MFM structure is applied an alternative voltage, either sinusoidal or triangular. The equivalent circuit in this case is formed by a capacitance – resistance parallel connection C_F-R_F, where C_F is the capacitance and R_F is the resistance of the ferroelectric volume, in series with a C_S capacitance associated to the Schottky contacts and a R_c resistance associated to metal contacts [26]. The real and imaginary parts of the impedance of this equivalent circuit, assuming a sinusoidal signal applied on the MFM structure, are given by:

$$Z' = \frac{R_c(\omega^2\tau_F^2+1)+R_F}{\omega^2\tau_F^2+1} \quad (1')$$

$$Z'' = \frac{1+\omega^2\tau_F(C_SR_F+\tau_F)}{\omega C_S(\omega^2\tau_F^2+1)} \quad (1'')$$

Here ω is the pulsation of the small amplitude a.c. signal ($\omega = 2\pi f$, with f the measuring frequency) and τ_F is the time constant for the ferroelectric layer ($\tau_F = C_FR_F$). Depending on the product $\omega\tau_F$, there can be two extreme cases:

$$\omega\tau_F >> 1 \text{ leading to } Z' = R_c + \frac{1}{\omega^2C_F^2R_F} \text{ and } Z'' = \frac{1}{\omega}\left(\frac{1}{C_F}+\frac{1}{C_S}\right) \quad (2')$$

$$\omega\tau_F << 1 \text{ leading to } Z' = R_c + R_F \text{ and } Z'' = \frac{1}{\omega}\left(\frac{1}{C_S}+\omega^2C_FR_F^2\right) \quad (2'')$$

For a given ω, one can be in one or the other of the cases depending on the values R_c, R_F, C_F and C_S. R_c is the resistance of the metallic contacts and it is expected to be low, maybe few hundreds of Ω. R_F is the d.c. resistance of the ferroelectric layer, while C_F is the capacitance for saturated polarization, not voltage dependent. C_S is the capacitance of the Schottky contacts, which is voltage dependent, increasing for forward bias (depletion region is reduced) and decreasing for reverse bias (depletion region is enlarged). R_c is not related to the structural quality of the MFM stack, but R_F and C_F are. C_S can be also affected by the structural quality, through the density of the free carriers (that can be reduced in a defective layer compared to the one in a layer of high epitaxial quality).

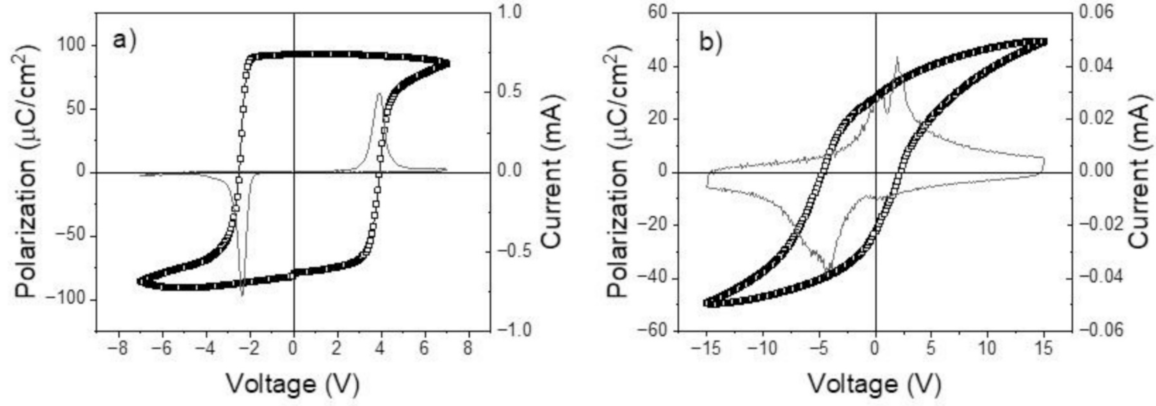

Fig. 1. Polarization and current hysteresis loops recorded for MFM structures based on an epitaxial (a) and on a polycrystalline (b) PZT film with Zr/Ti ratio on 20/80 Measurements performed in the dynamic mode, at 1 kHz.

One can simplify eqs. (2') and (2") even further, based on usual values for quantities involved in these equations. For simplicity, only high quality epitaxial films of perovskite ferroelectrics will be considered, to eliminate perturbative, extrinsic, contribution of structural defects that are present in textured or polycrystalline layers of the same materials. The C_F value is of the order of 100 pF [26]. It is more difficult to estimate R_F. This is because of the presence of the Schottky contacts at the electrode interfaces. It is largely accepted at present that a MFM structure is a back-to-back connection of two Schottky diodes (included in the equivalent circuit discussed above) [27,28]. For any polarity of the applied voltage, one diode is reversed biased, limiting the current flowing through the MFM structure, while the other is forward biased. However, in the case when there is only one Schottky contact and the other one is ohmic, for the voltage polarity when the Schottky contact is forward biased one ca presume that both contacts are ohmic and the ferroelectric layer is a resistor. Taking the current recorded in this case one can estimate a value between 10 and 100 KΩ for R_F [29]. Then the C_FR_F product, which is τ_F, is of the order of 10^{-6}–10^{-5} s. The usual frequency for hysteresis measurements is in between 10 and 1000 Hz. It results that the product $\omega\tau_F$ is at most 10^{-1}, much lower than unity. It means that, for usual conditions of the hysteresis measurements, the eq. (2") applies. $R_F >> R_c$, thus Z' can be approximated with R_F. The term $\omega^2 C_F R_F^2$ can be estimated to about 10^8 for a frequency of 1000 Hz, a C_F of 100 pF and a R_F of 100 kΩ. C_S is of the same order of magnitude as C_F, but during switching C_S can be significantly larger than C_F because the depletion region is very thin at both electrodes (one turns from reverse to forward biased, the other one turns from forward to reverse biased). The bottom line is that Z" is of the order of 10^8, much larger than Z'. In these conditions, the current flows mostly through the resistive branch of the parallel R-C circuit associated to the ferroelectric volume. Therefore, the entire MFM structure has a resistive like behavior during polarization switching.

II.2. Theory-Leakage current through a metal-ferroelectric-metal structure.

It was previously shown that the current density in MFM structures is governed by the following equation, which is a derivative of the thermionic emission over a potential barrier, taking into account the presence of the image charge (Schottky effect) and a mean free path of electrons smaller than the thickness of the sample [30–32]:

$$J = 2q\left(\frac{2\pi m_{eff}kT}{h^2}\right)^{3/2}\mu E exp\left(-\frac{q}{kT}\left(\Phi_B^0 - \sqrt{\frac{qE_m}{4\pi\varepsilon_0\varepsilon_{op}}}\right)\right) \tag{3}$$

The notations are as follows: m_{eff}-effective mass of electron; q-electron charge; k-Boltzmann's constant; T-temperature; h-Planck's constant; μ-electron mobility; *E*-applied electric field; P-polarization; ε_0-vacuum permittivity; ε_{op}-dielectric constant at optical wavelengths; Φ_B^0-the potential barrier at zero applied voltage; E_m-maximum electric field at the electrode interface assumed to behave as a Schottky contact. E_m is given by:

$$E_m = \sqrt{\frac{2qN_{eff}(V+V_{bi}')}{\varepsilon_0\varepsilon_{st}}} + \frac{P}{\varepsilon_0\varepsilon_{st}} \tag{4}$$

Where ε_{st}-static dielectric constant; N_{eff}-the effective density of charges in the depleted region (those charges that can respond to a small amplitude a.c. voltage during the capacitance measurement); V-the applied voltage; V_{bi}-the built-in potential in the presence of polarization charges.

Introducing (4) in (3), one obtains the following equation for the current density:

$$J \sim exp\left(-\frac{q}{kT}\left(\Phi_B^0 - \sqrt{\frac{q}{4\pi\varepsilon_0\varepsilon_{op}}\left(\frac{P}{\varepsilon_0\varepsilon_{st}} + \sqrt{\frac{2qN_{eff}V}{\varepsilon_0\varepsilon_{st}}}\right)}\right)\right) \tag{5}$$

V_{bi}' was neglected compared to the applied voltage.

Eq. (5) shows that the current density flowing through a MFM structure is modulated by the ferroelectric polarization through the height of the potential barrier at the electrode interfaces behaving as Schottky contacts. Technically, the exponent in eq. (5) can be very small when the switching begins, but polarization is still high and the applied voltage closes the coercive value [30]. [31] One can make a rough estimation using data reported in the literature for epitaxial PZT films: P about 1C/m^2, ε_{op} of 6.5, ε_{st} of 30 (the background dielectric constant), N_{eff} of 10^{25} m^{-3} and Φ_B^0 about 1 eV [26,28,30,33]. The exponent can be below 0.1 for example, and the exponential term is close to unity, in which case, the eq. (3) becomes:

$$J = 2q\left(\frac{2\pi m_{eff}kT}{h^2}\right)^{3/2}\mu E \tag{6}$$

Eq. (6) suggests that, for a limited time and voltage range during the polarization switching, the leakage current has an ohmic-like ($J = \sigma E$) behavior and the ferroelectric films behaves like a resistor, with a resistance that can be obtained from the slope of a current-voltage (I-V) characteristic, if this is linear (ohmic behavior).

The above considerations show that, during the polarization switching, the MFM structure may behave as a resistor and not as a capacitor, as suggeste also from considerations on the equivalent circuit discussed in the previous sub-section. All these considerations were made disregarding the strctural quality of the ferreoelctric. This can have a severe impact on the hysteresis measurements, as will be shown in the next sub-section.

II.3. Impact of structural quality on hysteresis.

Fig. 1 presents the results of the hysteresis measurements performed

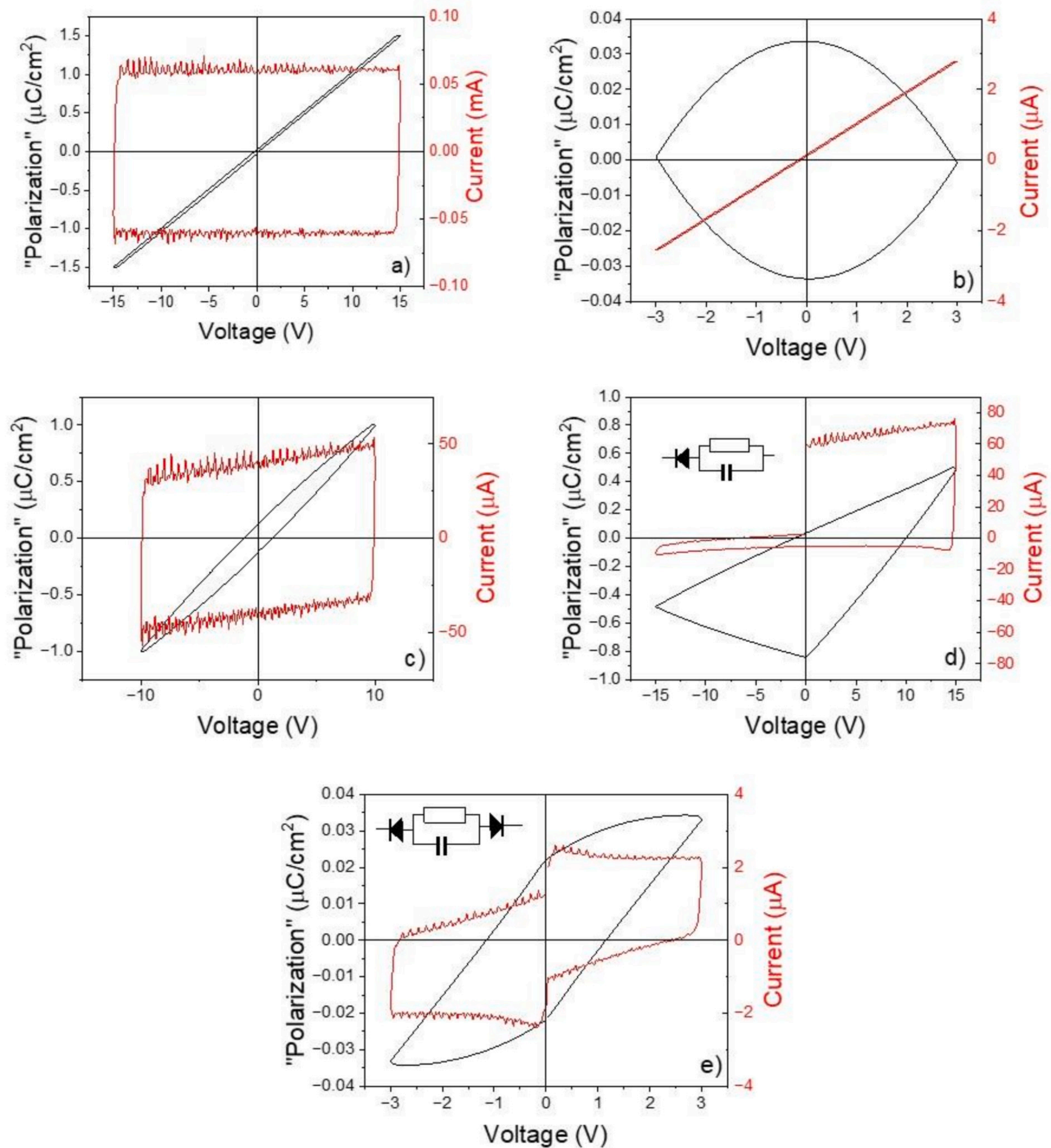

Fig. 2. "Polarization" and current hysteresis loops recorded for: a) commercial capacitor; b) commercial resistor; c) capacitor and resistor, parallel connection; d) a commercial Schottky diode connected to a parallel capacitor-resistor connection (see the inset); e) back-to-back Schottky diodes with a parallel capacitor-resistor connection in between (see the inset).

on two layers of $Pb(Zr_{0.2}Ti_{0.8})O_3$, with thicknesses of about 200 nm, one epitaxial prepared by pulsed laser deposition (PLD) on $SrRuO_3/SrTiO_3$ substrate, and one polycrystalline deposited by sol-gel on Pt/Si substrate. Details about deposition can be found elswehere [16].

One can observe large differences in the shape of the hysteresis and in the values of remnant polarization, coercive voltage and current. These results underline how crucial is the structural quality when assessing the material properties and polarization switching behavior. Such aspects cannot be included in simple models based on equivalent circuits, leakage current mechanisms or thermodynamic theories, all considering a MFM structure as a ferroelectric slab with two metal electrodes on it, without any indication on the influence of the structural quality.

However, based on the above results, one can hypothesize that an epitaxial film behaves more like a resistor, while a polycrystalline film behaves more like a capacitor, both having the equivalent circuit described in sub-section 1, only with different values for C_F, R_F, C_S, and the same eq. (4) for the current density, but with different values for P, N_{eff} and, possibly, ε_{st} (this is a discussion beyond the purpose of this study, concerning if the background dielectric constant of the ferroelectric should be used or the effective one derived from capacitance measurements).

The differences in Fig. 1, between the epitaxial and the polycrystalline films, can be attributed to grain boundaries. In a very good quality epitaxial film one has only electrode interfaces. In a polycrystalline film, besides the electrode interfaces one has those grain

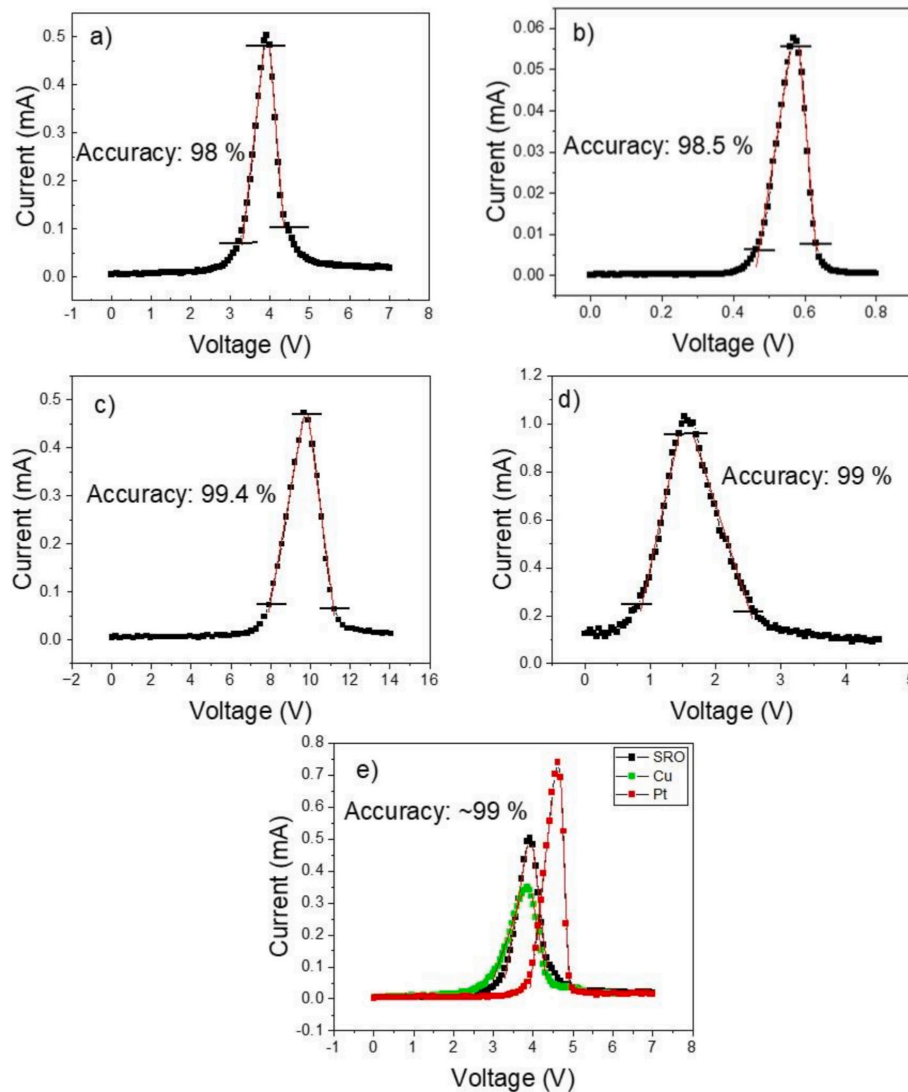

Fig. 3. The current peak associated to polarization switching for: a) PZT epitaxial layer with top and bottom SRO contacts; b) BTO epitaxial layer with top Pt and bottom SRO contacts; c) BFO epitaxial layer with top and bottom SRO electrodes; d) HZO layer with TiN electrodes; e) PZT epitaxial layer with bottom SRO contact and top SRO, Cu, and Pt electrodes. The red lines show the linear fit for the increasing and decreasing parts of the current peak; the horizontal black lines show the starting and ending points for the linear fit. The term Accuracy refers to the deviation from a perfect linear fit (see also Figure SM1). (For interpretation of the references to colour in this figure legend, the reader is referred to the web version of this article.)

boundaries that can introduce space charge regions, internal electric fields and other structural defects acting as traps or scattering centers for the free carriers, or impeding the polarization switching and the movement of the domain walls. The result is a lower current value, thus a larger resistance, and lower values for remnant polarization due to back-switching induced by local electric fields.

The results in Fig. 1 also suggests that the presence of the Schottky contacts at the electrode interfaces may be essential for the stability of polarization in epitaxial films, while in polycrystalline ones the presence of very good Schottky contacts at electrodes is not so critical due to the presence of a multitude of potential barriers at grain interfaces. Several experimental simulations were performed to verify this hypothesis.

II.4. Artificial simulation of MFM structures.

Test were performed using simple circuit components like resistors, capacitors and Schottky diodes, using the same equipment used for hysteresis measurements in the case of real MFM structures, namely TF2000 tester for ferroelectrics from AixACCT. In fig. 2 are presented the “polarization” and current hysteresis loops obtained in the following cases: simple capacitor (1 nF); simple resistor (1 MΩ); parallel capacitor-resistor circuit; parallel capacitor-resistor circuit in series with one Schottky diode; parallel capacitor-resistor circuit in series with two Schottky diodes connected back to back to mimic the equivalent circuit of a real MFM structure, as described in sub-section II.2. A triangular voltage wave of 1 kHz was applied on the “samples” in all cases. An area of 1 mm^2 was considered in all cases to calculate the so called “polarization”.

In the case of a capacitor (Fig. 2a), the “polarization” charge is proportional with the applied voltage, in the case of a resistor (Fig. 2b) the current is proportional with the applied voltage. For a parallel connection of a capacitor and resistor (Fig. 2c) the hysteresis is one expected for a leaky capacitor. If a Schottky diode is added at one side (Fig. 2d), the current is low when the Schottky diode is reverse biased and high when the diode is forward biased. When Schottky diodes are added on the both sides of the parallel connection of a capacitor and resistor (Fig. 2e) then one obtains a hysteresis loop similar to a MFM structure with a polycrystalline ferroelectric (see Fig. 1b for comparison).

These results demonstrate that both assumptions made in sub-

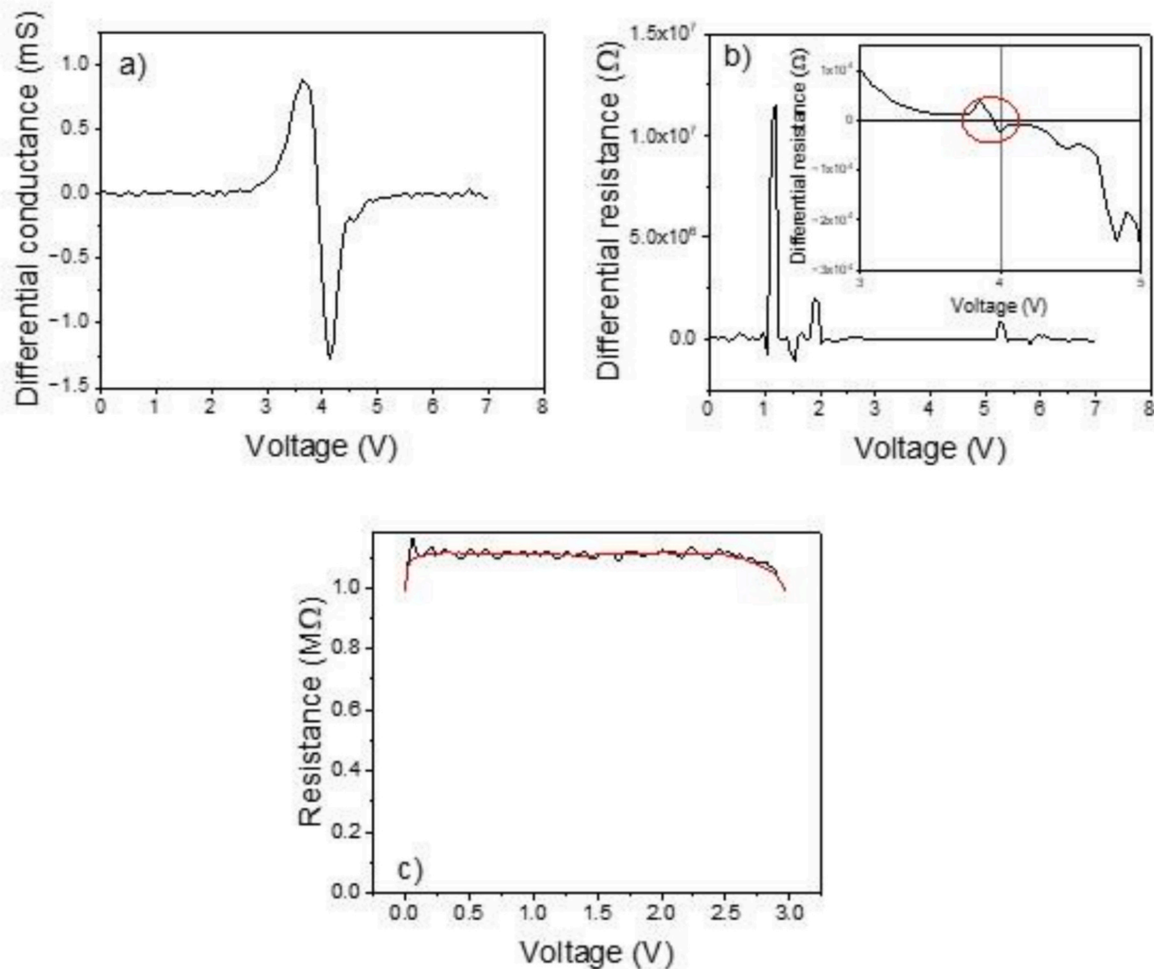

Fig. 4. a) Differential conductance obtained as the derivative of the I-V characteristic (peak) recorded during polarization switching; b) Differential resistance obtained as the derivative of the V—I characteristic, the inset shows the change in sign when polarization switching takes place (polarization changes orientation); c) Differential resistance obtained as the derivative of the V—I characteristic recorded for a commercial resistor.

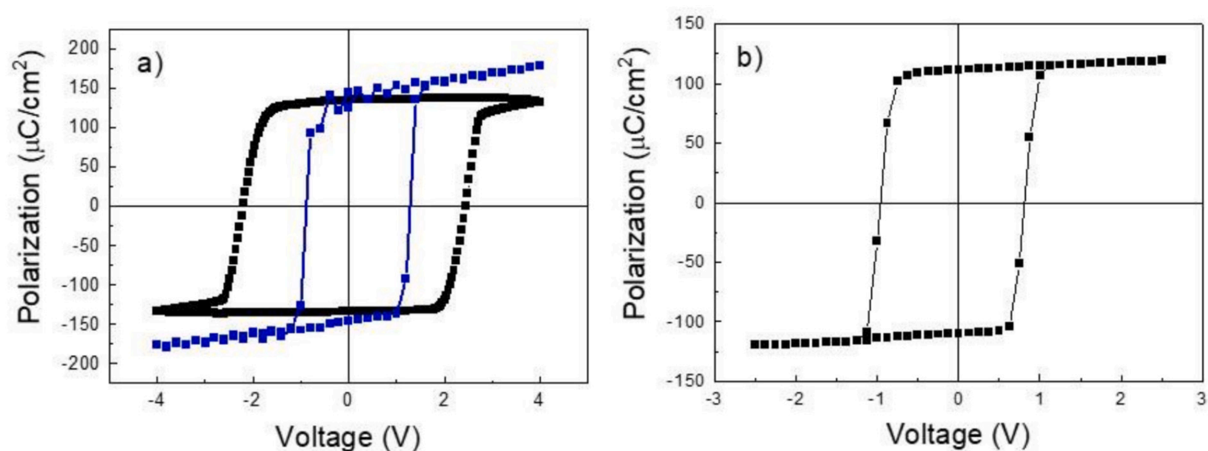

Fig. 5. a) Dynamic and static hysteresis recorded for a PZT film of 200 nm with top and bottom SRO electrodes; b) the static hysteresis recorded for a PZT film of 200 nm with bottom SRO and top Cu contacts. In both cases the PZT films were grown on STO single crystal substrates and were of high epitaxial quality. The hysteresis loops were recorded using a TF2000 ferroelectric analyzer, operating either in the dynamic or in static mode (details can be found in the operation manual).

sections II.1. and II.2. are correct, the equivalent circuit of a MFM structure is the one schematically shown in the inset of Fig. 2e, and the electrode interfaces behaves as Schottky contacts. In both cases it is predicted that the MFM structure may behave more like a resistor during polarization switching. However, this resistive like behavior can be influenced by the structural quality of the ferroelectric layer being, most probably, more pronounced for epitaxial films compared to poly-crystalline ones, when the capacitive behavior starts to dominate as

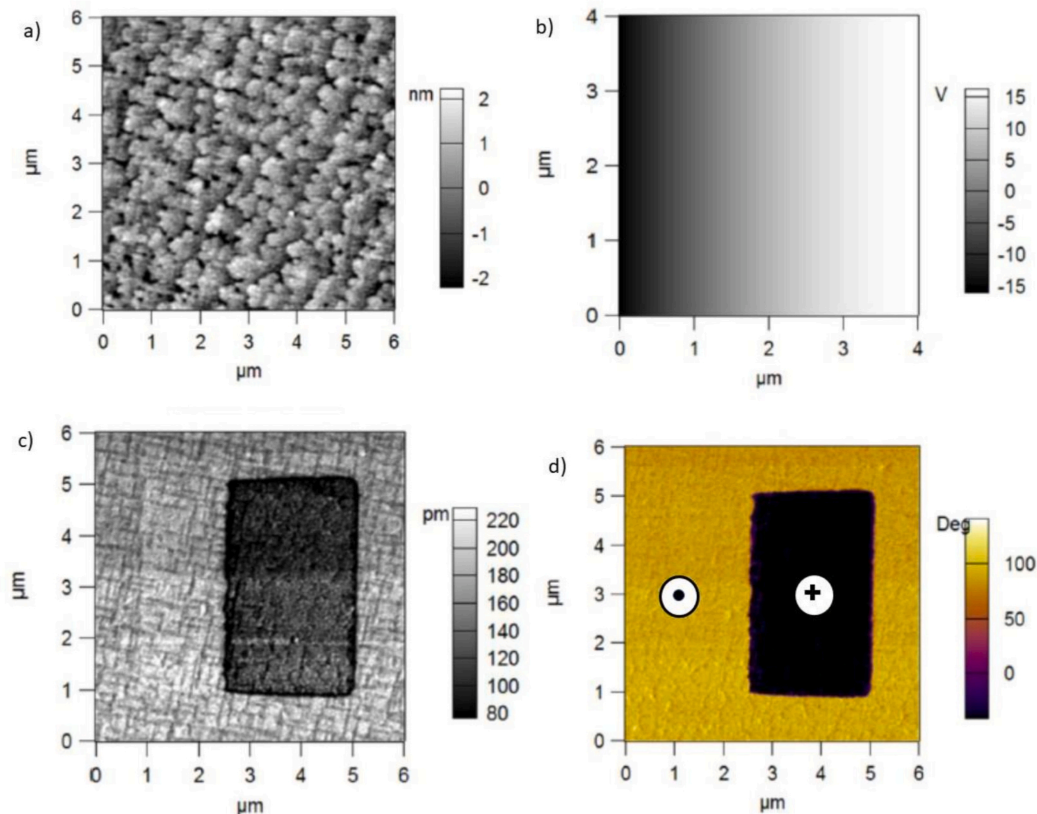

Fig. 6. PFM experiments on an epitaxial PZT film of 200 nm. a) topography; b) poling map; c) amplitude of the PFM signal; d) phase of the PFM signal. The black point inside a circle represents the point of the polarization orientated UP, while the cross represents the polarization orientated DOWN.

shown in sub-sections II.3. and II.4. Further on, the current behavior during polarization switching will be investigated in more detail.

3. Experimental methods

This work discus results of hysteresis measurements performed in the last 10 years on a variety of MFM samples from different ferroelectric materials, prepared by different methods, and using different electrodes. One can divide these samples in several groups:

1. PZT samples. The Zr/Ti ratio was 20/80. Most of the samples are epitaxial and were grown by PLD on $SrRuO_3/SrTiO_3$ substrates, with $SrRuO_3$ (SRO) acting as bottom electrode (about 20 nm thick). $SrTiO_3$ (STO) substrate is single crystal with (001) orientation. The top electrode was also SRO, but other metals were also used such as Cu or Pt. Some films were deposited by sol-gel on Pt/Si substrate, as mentioned in sub-section II.3. The thickness was, in general, around 200 nm and area of the top contacts was $100 \times 100\ \mu m^2$ if no other specific information is given. Information about the growth can be found in previous literature [16,28].
2. Other ferroelectrics with perovskite structure, such as $BaTiO_3$ (BTO) and Mn-doped $BiFeO_3$ (Mn-BFO) gown by PLD on STO/SRO substrates. Information about the growth can be found in previous articles [28].
3. Zr-doped HfO_2 (HZO) films grown by magnetron radio-frequency (RF) sputtering on Si substrate with TiN bottom electrode. Information about the growth can be found in previous articles [34].

All the electrical measurements were performed in cryogenic station from Lake Shore, with micromanipulator arms and CuBe needles to contact the MFM structure. For the hysteresis measurements, a TF2000 analyzer was used, as mentioned in sub-section II.4.

4. Experimental results of current hysteresis measurements

Fig. 3a depicts the current peak associated to polarizations switching for the PZT sample with polarization and current hysteresis shown in Fig. 1a. One can see that for a voltage range located between 3.2 and 4 V the I-V characteristics is linear, with a confidence factor around 99 % (see Figure SM1 in Supplementary Material – SM). One can assume that, in this voltage range, the MFM structure behaves mostly like a resistor, as discussed in sub-sections 2.1. and 2.2. This means that eq. (4) may apply in this case, meaning that the exponent is close to zero.

Fig. 3b), c) d) and e) presents similar results obtained on BTO, Mn-BFO, HZO, and PZT with different top electrodes, respectively (full polarization and current hysteresis loops are shown in Figures SM2-SM5). In all cases the increasing part of the current peak associated to the polarization reversal has a linear behavior with positive slope, as for the case of PZT. Even for polycrystalline films the increasing part of the current peak associated to polarization switching has a reasonable linear behavior, as can be seen in Fig. 1b) and detailed in SM-Figure SM6. However, the capacitive behavior is dominant over the resistive one. One can assume that this change is due to the many grain interfaces that impact the injected chares into the film, as will be discussed later on in section 5.

The linear behavior was observed for different temperatures, as well as for different amplitudes and frequencies of the triangular voltage wave used for hysteresis measurements. The temperature, amplitude and frequency dependencies of the resistance extracted from the increasing part of the current peak associated to polarization reversal are analyzed in more detail in SM for the case of PZT and HZO layers. The results suggest some common patterns but further studies are needed to fully explain these dependencies.

The decreasing part of the I-V characteristics in Fig. 3 has also a linear behavior, in all cases, but with a negative slope, meaning negative

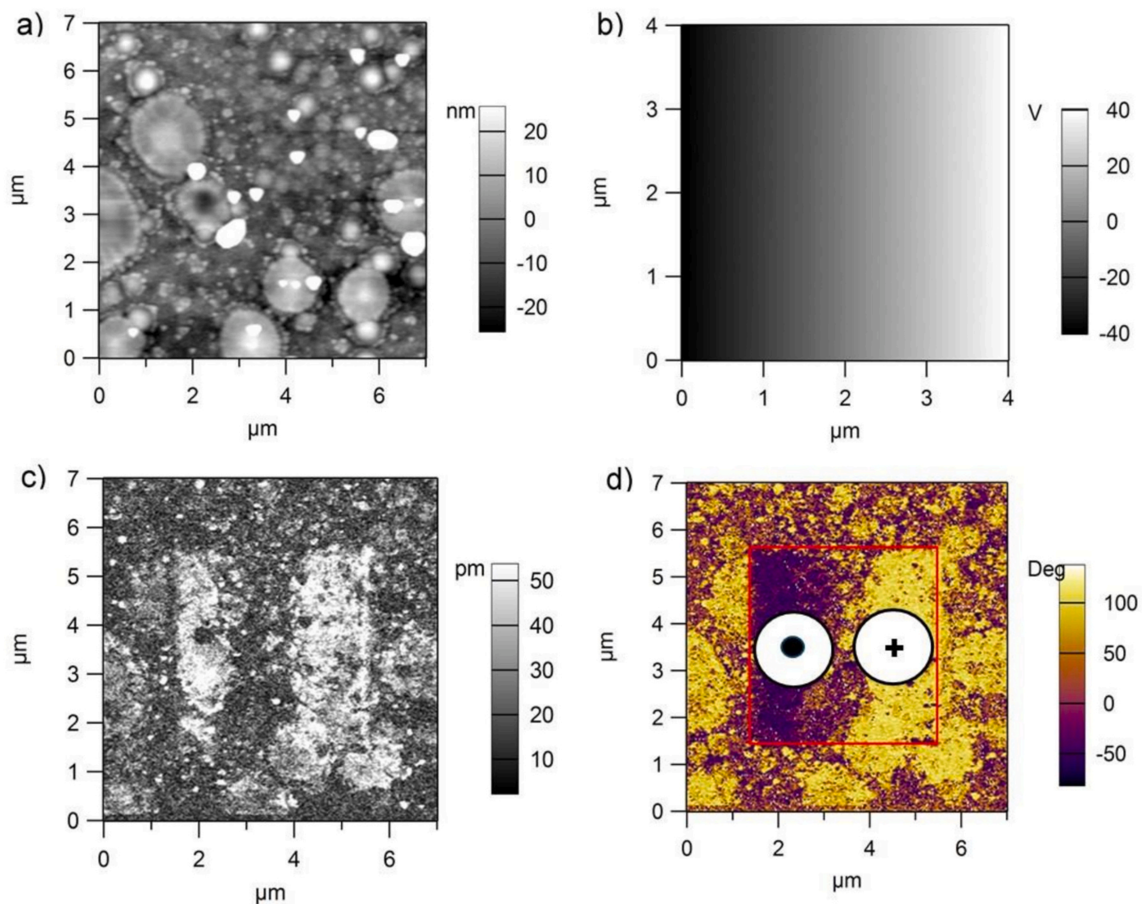

Fig. 7. PFM experiments on a polycrystalline PZT film of 200 nm. a) topography; b) poling map; c) amplitude of the PFM signal; d) phase of the PFM signal. The black point inside a circle represents the point of the polarization orientated UP, while the cross represents the polarization orientated DOWN.

conductance (or resistance). If the resistive like behavior with a positive value of conductance/resistance is supported by the theoretical considerations made in sub-section 2.1. and 2.2., the negative conductance/resistance extracted from the decreasing part of the current peaks in Fig. 3 is harder to explain but not impossible. These results will be approached in more detail in the next section.

5. Discussion

To shed some light on this matter, one should refer to the differential resistance and not to the one related to the linear current-voltage characteristic encountered in the case of a simple resistor. One can take into consideration that the polarization switching is a dynamic effect, implying not only the switch of bound polarization charges from one electrode interface to the other, but also the change of the charges involved in the compensation of the depolarization field associated to ferroelectric polarization, whatever these are free or trapped charges. Therefore, polarization switching implies not only the displacement current dP/dt (P being the polarization and t the time), but also transitory currents produced by the redistribution of the charges involved in the compensation of the newly generated depolarization field associated to the new orientation of polarization after switching. A differential resistance may be recommended in this case of transient currents. This is supported by the fact that negative differential resistance (NDR) was reported in structures involving ferroelectric layers [35–38]. In the followings only PZT films will be considered, assuming that the conclusions drawn in this case apply to other similar oxide ferroelectrics.

5.1. *Differential resistance/conductance*

The direct derivative of the current-voltage (I-V) characteristic shown in Fig. 3a) gives, in fact, the differential conductance G = dI/dV. The obtained graph is shown in Fig. 4a). However, it is not straightforward that the differential resistance is the reverse of the differential conductance. To directly obtain the differential resistance, the I-V characteristic was transformed in a V—I one (it is actually a 90-degree clockwise rotation of the graph in Fig. 3a) then the derivative was extracted. The result is presented in Fig. 4b). One can see that the differential resistance is much noisier that the differential conductance, probably because of large noise in current at voltages for which the current values are small (below 3 V and above 5 V). Therefore, only the voltage range between 3 and 5 V was considered and presented in the inset of Fig. 3b). It is the voltage range corresponding to polarization switching.

The inset shows that at a voltage slightly below 4 V (corresponding to the current peak in Fig. 3a), the differential resistance change from positive to negative and remains negative until the switching ends. Similar behavior has the differential conductance, who becomes negative at voltages larger than, roughly, 4 V. For voltages below 3 V and above 5 V the differential resistance has an average value of about 200 kΩ, significantly larger than in the voltage range where the switching take place.

These results are somewhat contrary to one have expected from considerations in sub-sections II.1. and II.2., and from the linear behavior of the current on the increasing and decreasing parts of the peak associated to polarization switching, all suggesting a resistor like behavior with an ohmic like I-V characteristic similar to a standard

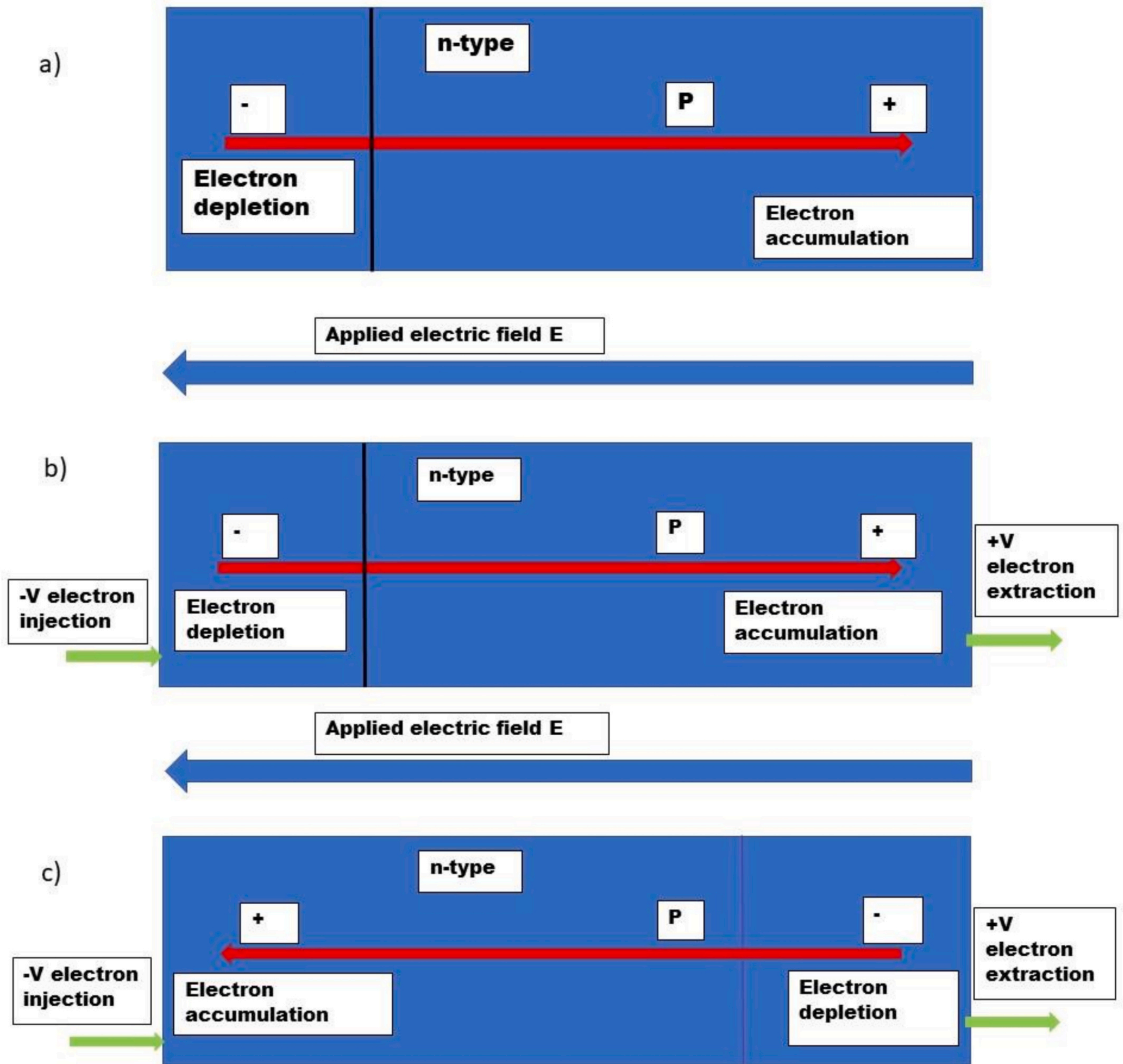

Fig. 8. a) The initial state of the MFM structure, with electrodes on the left and right sides of the blue slab mimicking the ferroelectric layer, the initial orientation of polarization is indicated by the red arrow; b) An external electric field (see the blue arrow above the ferroelectric slab) is applied opposite to the initial direction of polarization. Charges start to be injected at electrode interfaces as indicated by the green arrows; c) The state of the MFM structure after polarization switching, when polarization's orientation is parallel with the applied field. (For interpretation of the references to colour in this figure legend, the reader is referred to the web version of this article.)

resistance. For completeness, the derivative of the V—I characteristic (see Fig. 2b) is shown in Fig. 4c). One can see that, disregarding the inherent noise of the derivative, the resistance value is constant with voltage and about 1 MΩ within an error of 10 %, which is the tolerance of the commercial resistance used in the experiments of sub-section II.4. By contrast, the differential resistance and the differential conductance have a resonant like behavior at switching. Some other interesting features observed for the increasing part of the current peak are discussed separately in SI.

This behavior will be explained, at least qualitatively, proposing that the polarization switching is triggered by charge injection/extraction at interfaces, without domain formation in high quality crystals, the domains occurring in imperfect crystals as will be explained later on. The new model is taking into consideration the presence of the Schottky like contacts at electrode interfaces and the preliminary considerations from sub-section II.1. and II.4.

5.2. Relation between structural quality and domain formation during switching

The classic theories of switching are based on nucleation and growth of ferroelectric domains [39]. When polarization is saturated, on a direction or the other, the ferroelectric is monodomain, with polarization oriented up or down. The switching starts with nucleation of domains

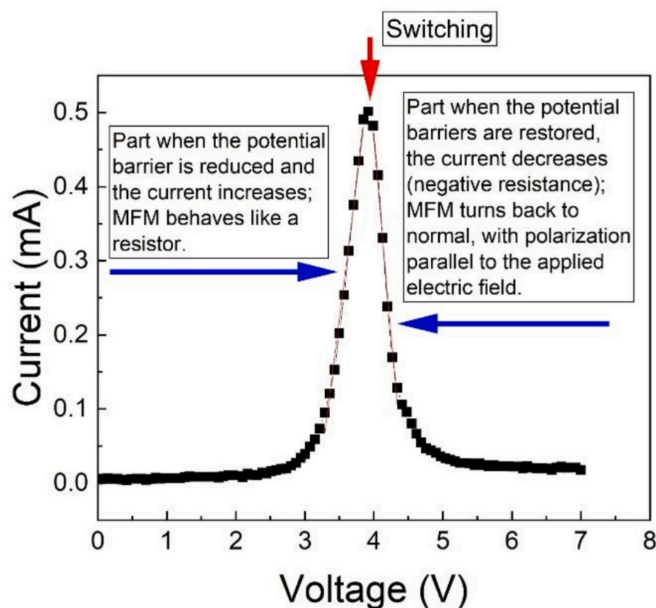

Fig. 9. The origin of the current peak at polarization switching in relation to the behavior of potential barriers at interfaces in the MFM structure schematically presented in Fig. 8.

with opposite direction of polarization, and the state with zero polarization (at coercive fields +/− E_c) is obtained when there are equal volumes with up and down polarization. In terms of thermodynamic theory, the switching is explained based on the double well free energy landscape, as in [40].

Domain formation and charge injection at interfaces does not exclude each other, especially in highly defective films, where they can coexist and influence each other's as for example through conductive domain walls. However, as the structural quality increases towards single crystal and only electrode interfaces remain, the probability that polarization switching takes place through domain formation decreases, the switching being dominantly triggered by charge injection as proposed in the previous section. There are some experimental evidences supporting this claim. For example, the hysteresis loops presented in Fig. 5.

One can see that in the static mode there are only a few intermediate polarization states between the extreme up and down values. This finding suggests that if domains are forming, these are only a few and rapidly expanding to the entire volume, so that the switching is very abrupt in the static hysteresis loop.

An even more relevant experiment is to use PFM for switching. Fig. 6b shows a poling map in which the applied voltage on the tip was increased from -15 V to +15 V while the tip was scanned on the surface from left to right. Fig. 6c) shows the phase variation recorded when the above-mentioned poling map was used. One can see that the phase suddenly changes when polarization switches from up (bright surface) to down (dark surface). This result suggests that, when coercive voltage is achieved, the polarization switches from up to down in the entire volume.

This experiment also confirms that as-grown PZT epitaxial films are having up polarization if grown on SRO electrode [41].

The situation is totally different in a polycrystalline film deposited by sol-gel on a Pt/Si substrate [16], as shown in Fig. 7. Using a similar poling map, one can see that the switching is gradual (see the red square in Fig. 7d). The two opposite directions of polarization are separated by a zone where domains of opposite orientations co-exist. There are also small areas where the polarization does not switch, suggesting that the local electric fields due to charged structural defects are strong enough to prevent switching.

5. 3. The model of polarization switching triggered by charge injection at interface.

The previously presented experimental findings can be explained starting from the schematic shown in Fig. 8 and the hypothesis that the polarization switching is triggered by charge injection at the electrode interfaces.

In Fig. 8a) the MFM structure is in a well-defined polarization state (polarization is considered saturated), so that the compensation of the depolarization field requires accumulation of electrons at the electrode interface where the polarization charge is positive (right side in Fig. 8a), and depletion of electrons at the opposite electrode interface, where the polarization charge is negative (left side in Fig. 5a). One can say that the left interface is a reverse biased Schottky contact, while the right interface is a forward biased. However, the charges compensating the depolarization field are somehow blocked at the interfaces, possibly on interface traps, otherwise a cure would be detected in an external circuit, which is not the case, the MFM structure does not act as a charged capacitor, that generates a current when short-circuited.

In Fig. 8b) an external electric field is applied on the MFM structure, opposing the direction of polarization. Electron will be injected at the left interface, reducing the depletion region, and will be extracted at the right interfaces (green arrows in Fig. 8b). As the voltage increases, more electrons will be injected and extracted at electrode interfaces, the consequence being the destabilization of the charges that compensate the depolarization filed. The final result is that the polarization is no longer stable on the initial orientation and has to switch on the direction of the applied field (see also the Fig. 9, relating what happens with the potential barriers at interfaces with the current peak at switching). During this process, the barriers at interfaces may disappear and the current flowing through the MFM structure may have an ohmic like behavior as function of the applied voltage, as suggested by eq. (4) in sub-section II.2. This can explain the increasing part of the current peak in Fig. 3a).

Further on, in Fig. 8c) is presented the situation after polarization switching. Electrons continue to be injected at left interface, but this time they contribute to the compensation of the positive polarization charges and extracted at the right interface, building a depletion region and compensating the negative polarization charges. At the end, a reverse biased Schottky like contact appear at the right interface, limiting the current through the entire MFM structure. The current decreases as the depletion region increases, leading to the decreasing part of the current peak in Fig. 3a) and the negative differential resistance or conductance (see also Fig. 9). At the end, the polarization is saturated and stabilized by the compensation charges located in the interface regions and the current returns to low values recorded before switching (see Fig. 3a) below 3 and above 5 V).

In the above discussion it was assumed that the PZT films is n-type (we remind that it is an epitaxial film) due to the presence of oxygen vacancies, but the discussion remains valid for a p-type ferroelectric as long as there are Schottky like contacts at the electrode interfaces.

The I-V characteristics presented in Fig. 3 where all obtained on high quality epitaxial films. Looking at Fig. 2b), one can see that NDR is present also in polycrystalline films, since there is also a decreasing part of the current peak associated to polarization switching. The current peak in this case is broader due to back switching effects. The compensation process of the depolarization filed after switching is more complicated in this case, one can have a distribution of local electric fields, potential barriers at different heights and widths, more traps, all making the capacitive like behavior more pronounced, but still at switching the resonant like behavior of NDR remains.

The explanation given above in relation to Fig. 8 remains valid only that it applies to all the grain barriers, not only to the electrode interfaces, as shown in Fig. 10.

The schematic in Fig. 10 may look over-simplified but it helps to understand the switching in polycrystalline samples assumed to be a collection of perfect crystals, with different orientations of polarization

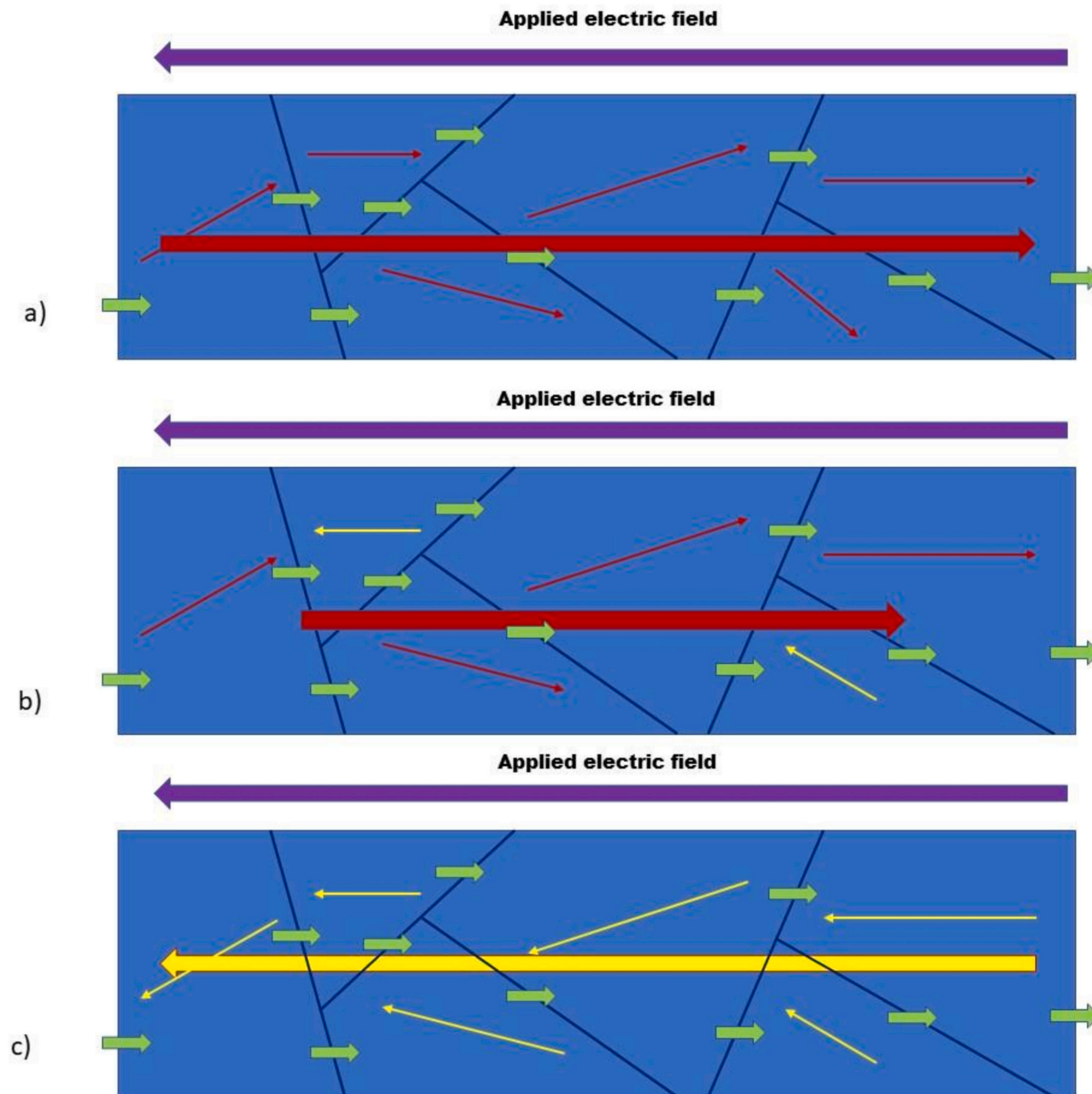

Fig. 10. The schematic of the of the polarization switching triggered by charge injection/extraction at interfaces in a polycrystalline sample. Narrow red arrows show initial direction of polarization in different crystalline grains assumed to be perfect crystals, and the thick red arrow show the initial direction of polarization at macroscopic scale before switching. Yellow arrows show polarization direction after switching. Green arrows show the charge flow at interfaces, injection on one side and extraction on the other side. A) is the situation before switching, just when an external field is applied on the sample; b) show an intermediate situation, when polarization has switched in some grains; c) is the final state, after switching and when polarization is saturated in the direction imposed by the external electric field. (For interpretation of the references to colour in this figure legend, the reader is referred to the web version of this article.)

and potential barriers at the interfaces between crystalline grains. In each grain there will be a polarization component perpendicular on the electrodes (lateral sides in Fig. 10), leading to a net polarization as schematically presented by the thick red arrow in Fig. 10a). When an electric field is applied charges start to be injected/extracted at each interface, leading to switching in different grains when the local condition for the compensation of the depolarization field is no longer fulfilled. As the field increases, polarization switches in more and more grains (intermediate situation in Fig. 10b) until it switches in all grains and the microscopic resultant is parallel to the applied electric field (see Fig. 10c).

When PFM is used, then only the component perpendicular to the surface is probed, leading to phase contrasts that are usually called domains. However, because of the structural defects, the switching is not sudden in all the volume, but it is gradual, leading to a more elongated hysteresis loop and to a broader current peak as shown in Fig. 3b).

At the end, a few words about the Landau-Khalatnikov (LK) equation, given by [19]:

$$\delta\frac{dP}{dt} = \frac{dG}{dP} \tag{6}$$

P is the polarization, t is the time, G is the free energy in the presence of an applied electric field E and δ is a kinetic coefficient. It is interesting to notice that dP/dt has the units of a current density, while dG/dP is an electric field, thus eq. (4) resembles the relation J = σE of an ohmic like conduction, similar to eq. (4). For G, the following equation is used:

$$G(P) = G_0 + \frac{1}{2}aP^2 + \frac{1}{4}bP^4 + \frac{1}{6}cP^6 - EP \tag{7}$$

G_0 is the free energy at zero electric field and a, b, c are thermodynamic coefficients. Introducing (7) in (6) and using a periodic electric field of the form $E_0\sin(\omega t)$ ($\omega = 2\pi f$, with f the frequency of the applied a.

c. signal for the hysteresis measurement), one can simulate practically any polarization or current hysteresis loop if one uses proper value for δ, P, a, b and c [19,42,43].

The problem with these thermodynamic models (and others) is that they do not take into consideration microstructural features, like potential asymmetry in electrode interfaces, local fields generated by charge defects, or mobile charge carriers. Although it may reproduce a hysteresis behavior, including a linear-like dependencies of the I-V characteristics on the increasing or decreasing parts of the current peak associated to polarization reversal, they cannot explain the asymmetries often encountered in real hysteresis loops, not mentioning the, sometimes large, differences observed in the hysteresis loops recorded for different samples from nominally the same material. They can simulate a general behavior, but not all details. This is an enormous task, going far beyond the scope of the present study.

At the end, a short discussion on polarization switching models in ferroelectrics. As mentioned in the Introduction section, the vast majority of the models assume that, when an external electric field as applied on a MFM structure in opposite direction to the polarization one, domains will nucleate and grow with polarization orientation parallel to the applied field and opposite to the initial orientation of it. Aside of the references mention in the Introduction, one can mention also the excellent review of Scott in [13]. Same author mentions also the possibility of polarization switching without domain formation, see Ref. [44]. In this reference it is mentioned that switching without domain formation is possible in perfect crystals, or at least nearly perfect, since domains tend to form on charged structural defects located in the volume or at interfaces, whatever these are at electrodes or between crystalline grains. Our findings show that, indeed, domains may for or not depending on the structural quality of the ferroelectric film.

In support to our model of polarization switching triggered by charge injection/extraction at interfaces, we would like to remind a phenomenon that was relatively intensive studied 10–15 years ago, namely electron emission from ferroelectric surfaces [45]. Electron emission takes place when there is a sudden change in polarization, e.g. at switching. It means that those charges are accumulated at the surface to compensate the bound polarization charges and when the sign of these charges changes, then the electrons are emitted. By extension, this can be regarded as a charge injection/extraction at the interface.

6. Conclusions

In conclusion, a new switching mechanism is proposed, based on charge injection/extraction at electrode or crystalline grain interfaces. It is also evidenced, both theoretically and experimentally, that the MFM structure during polarization switching has a resistive like behavior. The resistance is positive on the increasing part of the current peak associated to switching and negative on the decreasing part. This is explained qualitatively by the disappearance of the potential barrier at the electrode interface on one side (increasing part of the peak) and reappearance of the potential barrier at the opposite electrode interface (decreasing part of the peak). Similar effect may occur at grain boundaries that are in between electrode interfaces. The resistive like behavior seems to be present in oxide ferroelectrics, although the analyzed samples are of different materials, different thicknesses, different structural qualities and with different electrodes, this behavior being related only to the properties of the electrode or grain interfaces. However, the thickness of the ferroelectric layer may have some influence in the case of polycrystalline films, as well as the size of the grains, in the sense that these two quantities influence the number of gain interfaces between the electrodes. This will be subject of a future study.

Present results suggest that, in perfect MFM structures the switching takes place, most probably, without domain formation, being triggered by the imbalance of the depolarization field due to the injected/extracted charges up to the point when the polarization direction is no longer stable and has to orient parallel to the external electric field. Once the defects are present, then domains may form and the switching may be modeled by nucleation and growth, although down to single perfect crystalline grains the switching inside those gains takes place still without domain formation. Anyway, further studies are needed to confirm the model, implying pushing farther to obtain perfect MFM structures.

CRediT authorship contribution statement

Lucian Pintilie: Writing – review & editing, Writing – original draft, Validation, Supervision, Project administration, Funding acquisition, Formal analysis, Conceptualization. **Georgia Andra Boni:** Visualization, Validation, Methodology, Investigation, Formal analysis, Data curation. **Cristina Florentina Chirila:** Visualization, Validation, Methodology, Investigation, Data curation. **Luminita Mirela Hrib:** Visualization, Validation, Formal analysis, Data curation. **Lucian Trupina:** Visualization, Validation, Methodology, Investigation, Formal analysis, Data curation. **Cristian Mihail Teodorescu:** Writing – review & editing, Visualization, Validation, Formal analysis. **Athanasios Dimoulas:** Writing – review & editing, Visualization, Validation, Funding acquisition, Formal analysis, Conceptualization.

Declaration of competing interest

The authors declare that they have no known competing financial interests or personal relationships that could have appeared to influence the work reported in this paper.

Acknowledgments

The authors acknowledge financial support through the PNRR project 760239/28.12.2023, funded by the Romanian Ministry of Research, Innovation and Digitization through the National Recovery and Resilience Plan, and through the Core Program project PN23080202.

Appendix A. Supplementary data

Supplementary data to this article can be found online at https://doi.org/10.1016/j.mseb.2025.119130.

Data availability

Data will be made available on request.

References

[1] M.E. Lines, A.M. Glass, Principles and applications of ferroelectrics and related materials, Oxford University Press (2001), https://doi.org/10.1093/acprof:oso/9780198507789.001.0001.
[2] A.K. Bain, P. Chand, Ferroelectrics: Principles and Applications, Wiley VCH Verlag GmbH, Weinheim, Germany, 2017.
[3] J. Schwarzkopf, R. Fornari, Epitaxial growth of ferroelectric oxide films, Prog. Cryst. Growth Charact. Mater. 52 (2006) 159–212, https://doi.org/10.1016/j.pcrysgrow.2006.06.001.
[4] C.B. Eom, R.B. Van Dover, J.M. Phillips, D.J. Werder, J.H. Marshall, C.H. Chen, R. J. Cava, R.M. Fleming, D.K. Fork, Fabrication and properties of epitaxial ferroelectric heterostructures with (SrRuO3) isotropic metallic oxide electrodes, Appl. Phys. Lett. 63 (1993) 2570–2572, https://doi.org/10.1063/1.110436.
[5] B. Nagaraj, S. Aggarwal, R. Ramesh, Influence of contact electrodes on leakage characteristics in ferroelectric thin films, J. Appl. Phys. 90 (2001) 375–382, https://doi.org/10.1063/1.1371947.
[6] C. Sudhama, A.C. Campbell, P.D. Maniar, R.E. Jones, R. Moazzami, C.J. Mogab, J. C. Lee, A model for electrical conduction in metal-ferroelectric-metal thin-film capacitors, J. Appl. Phys. 75 (1994) 1014–1022, https://doi.org/10.1063/1.356508.
[7] P.W.M. Blom, R.M. Wolf, J.F.M. Cillessen, M.P.C.M. Krijn, Ferroelectric Schottky diode, Phys. Rev. Lett. 73 (1994) 2107–2110, https://doi.org/10.1103/PhysRevLett.73.2107.
[8] A.L. Kholkin, S.V. Kalinin, A. Roelofs, A. Gruverman, Review of ferroelectric domain imaging by Piezoresponse force microscopy, in: S. Kalinin, A. Gruverman (Eds.), Scanning Probe Microscopy: Electrical and Electromechanical Phenomena

at the Nanoscale, Springer, New York, NY, 2007, pp. 173–214, https://doi.org/10.1007/978-0-387-28668-6_7.
[9] L. Li, L. Xie, X. Pan, Real-time studies of ferroelectric domain switching: a review, Rep. Prog. Phys. 82 (2019) 126502, https://doi.org/10.1088/1361-6633/ab28de.
[10] U. Ludacka, J. He, S. Qin, M. Zahn, E.F. Christiansen, K.A. Hunnestad, X. Zhang, Z. Yan, E. Bourret, I. Kézsmárki, A.T.J. van Helvoort, J. Agar, D. Meier, Imaging and structure analysis of ferroelectric domains, domain walls, and vortices by scanning electron diffraction, npj Comput. Mater. 10 (2024) 106, https://doi.org/10.1038/s41524-024-01265-y.
[11] C.S. Tsang, X. Zheng, T.H. Ly, J. Zhao, Recent progresses in transmission electron microscopy studies of two-dimensional ferroelectrics, Micron 185 (2024) 103678, https://doi.org/10.1016/j.micron.2024.103678.
[12] D. Denning, J. Guyonnet, B.J. Rodriguez, Applications of piezoresponse force microscopy in materials research: from inorganic ferroelectrics to biopiezoelectrics and beyond, Int. Mater. Rev. 61 (2016) 46–70, https://doi.org/10.1179/1743280415Y.0000000013.
[13] J.F. Scott, A review of ferroelectric switching, Ferroelectrics 503 (2016) 117–132, https://doi.org/10.1080/00150193.2016.1236611.
[14] Y.A. Genenko, J. Wehner, H. von Seggern, Self-consistent model of polarization switching kinetics in disordered ferroelectrics, J. Appl. Phys. 114 (2013) 084101, https://doi.org/10.1063/1.4818951.
[15] X.J. Lou, Four switching categories of ferroelectrics, J. Appl. Phys. 105 (2009) 094112, https://doi.org/10.1063/1.3117494.
[16] L. Pintilie, G.A. Boni, C.F. Chirila, V. Stancu, L. Trupina, C.M. Istrate, C. Radu, I. Pintilie, Homogeneous versus inhomogeneous polarization switching in PZT thin films: impact of the structural quality and correlation to the negative capacitance effect, NANOMATERIALS 11 (2021), https://doi.org/10.3390/nano11082124.
[17] M.J. Highland, Polarization switching without domain formation at the intrinsic coercive field in ultrathin ferroelectric PbTiO3, Phys. Rev. Lett. 105 (2010), https://doi.org/10.1103/PhysRevLett.105.167601.
[18] S. Park, R. Kim, I.A. Young, Collective behavior in intrinsic polarization switching of PbTiO3 and Pb(Zr,Ti)O3, J. Appl. Phys. 136 (2024) 245104. doi:https://doi.org/10.1063/5.0234012.
[19] A.G. Maslovskaya, L.I. Moroz, A.Yu. Chebotarev, A.E. Kovtanyuk, Theoretical and numerical analysis of the Landau–Khalatnikov model of ferroelectric hysteresis, Commun. Nonlinear Sci. Numer. Simul. 93 (2021) 105524, https://doi.org/10.1016/j.cnsns.2020.105524.
[20] Y.-L. Wang, X.-Y. Wang, L.-Z. Chu, Z.-C. Deng, W.-H. Liang, B.-T. Liu, G.-S. Fu, N. Wongdamnern, T. Sareein, R. Yimnirun, Simulation of hysteresis loops for polycrystalline ferroelectrics by an extensive Landau-type model, Phys. Lett. A 373 (2009) 4282–4286, https://doi.org/10.1016/j.physleta.2009.09.050.
[21] P.D. Lomenzo, M. Materano, C. Richter, R. Alcala, T. Mikolajick, U. Schroeder, A Gibbs energy view of double hysteresis in ZrO2 and Si-doped HfO2, Appl. Phys. Lett. 117 (2020) 142904, https://doi.org/10.1063/5.0018199.
[22] N. Wongdamnern, A. Ngamjarurojana, Y. Laosiritaworn, S. Ananta, R. Yimnirun, Dynamic ferroelectric hysteresis scaling of BaTiO3 single crystals, J. Appl. Phys. 105 (2009) 044109, https://doi.org/10.1063/1.3086317.
[23] M. Zhang, C. Deng, Scaling behavior of dynamic hysteresis in epitaxial ferroelectric BaTiO3 thin films, J. Alloys Compd. 883 (2021) 160864, https://doi.org/10.1016/j.jallcom.2021.160864.
[24] D.J. Wouters, G. Willems, E.G. Lee, H.E. Maes, Elucidation of the switching processes in tetragonal pzt by hysteresis loop and impedance analysis, Integr. Ferroelectr. 15 (1997) 79–87, https://doi.org/10.1080/10584589708015698.
[25] I. Vrejoiu, G. Le Rhun, L. Pintilie, D. Hesse, M. Alexe, U. Gösele, Intrinsic Ferroelectric Properties of Strained Tetragonal PbZr0.2Ti0.8O3 Obtained on Layer–by–Layer Grown, Defect–Free Single–Crystalline Films, Adv. Mater. 18 (2006) 1657–1661, https://doi.org/10.1002/adma.200502711.
[26] L. Pintilie, L. Hrib, I. Pasuk, C. Ghica, A. Iuga, I. Pintilie, General equivalent circuit derived from capacitance and impedance measurements performed on epitaxial ferroelectric thin films, J. Appl. Phys. 116 (2014) 044108, https://doi.org/10.1063/1.4891255.
[27] H. Yang, H.M. Luo, H. Wang, I.O. Usov, N.A. Suvorova, M. Jain, D.M. Feldmann, P. C. Dowden, R.F. DePaula, Q.X. Jia, Rectifying current-voltage characteristics of BiFeO3/Nb-doped SrTiO3 heterojunction, Appl. Phys. Lett. 92 (2008) 102113.
[28] I. Pintilie, C.M. Teodorescu, C. Ghica, C. Chirila, A.G. Boni, L. Hrib, I. Pasuk, R. Negrea, N. Apostol, L. Pintilie, Polarization-control of the potential barrier at the electrode interfaces in epitaxial ferroelectric thin films, ACS Appl. Mater. Interfaces 6 (2014) 2929–2939, https://doi.org/10.1021/am405508k.
[29] L. Pintilie, Ferroelectric Schottky diode behavior from a SrRuO3-pb(Zr0.2 Ti0.8) O3-ta structure, Phys. Rev. B 82 (2010), https://doi.org/10.1103/PhysRevB.82.085319.
[30] L. Pintilie, I. Vrejoiu, D. Hesse, G. LeRhun, M. Alexe, Ferroelectric polarization-leakage current relation in high quality epitaxial PbZr,TiO3 films, Phys. Rev. B 75 (2007) 104103, https://doi.org/10.1103/PhysRevB.75.104103.
[31] L. Pintilie, Charge Transport in Ferroelectric Thin Films, in: Ferroelectrics - Physical Effects, IntechOpen, 2011, https://doi.org/10.5772/18165.
[32] Physics of Semiconductor Devices, 3rd edition, Wiley, 2025. Wiley.Com (n.d.), https://www.wiley.com/en-us/Physics+of+Semiconductor+Devices%2C+3rd+Edition-p-9780470068328. accessed September 22.
[33] G.A. Boni, C.F. Chirila, L. Hrib, R. Negrea, L.D. Filip, I. Pintilie, L. Pintilie, Low value for the static background dielectric constant in epitaxial PZT thin films, Sci. Rep. 9 (2019), https://doi.org/10.1038/s41598-019-51312-8.
[34] C. Zacharaki, P. Tsipas, S. Chaitoglou, S. Fragkos, M. Axiotis, A. Lagoyiannis, R. Negrea, L. Pintilie, A. Dimoulas, Very large remanent polarization in ferroelectric Hf1-xZrxO2 grown on Ge substrates by plasma assisted atomic oxygen deposition, Appl. Phys. Lett. 114 (2019) 112901, https://doi.org/10.1063/1.5090036.
[35] Y. Luo, J. Chen, A. Abbas, W. Li, Y. Sun, Y. Sun, J. Yi, X. Lin, G. Qiu, R. Wen, Y. Chai, Q. Liang, C. Zhou, Robust Giant tunnel Electroresistance and negative differential resistance in 2D semiconductor/α-In2Se3 ferroelectric tunnel junctions, Adv. Funct. Mater. 34 (2024) 2407253, https://doi.org/10.1002/adfm.202407253.
[36] X. Gan, Y. Zhang, Y. Hui, S. Liu, L. Wang, J. Zhang, Y. Hao, H.H. Ma, Controlling Memristance and negative differential resistance in point-contacted metal–oxides–metal heterojunctions: role of oxygen vacancy electromigration and Electron hopping, Adv. Intell. Syst. 4 (2022) 2200020, https://doi.org/10.1002/aisy.202200020.
[37] P. Li, Z. Huang, Z. Fan, H. Fan, Q. Luo, C. Chen, D. Chen, M. Zeng, M. Qin, Z. Zhang, X. Lu, X. Gao, J.-M. Liu, An unusual mechanism for negative differential resistance in ferroelectric nanocapacitors: polarization switching-induced charge injection followed by charge trapping, ACS Appl. Mater. Interfaces 9 (2017) 27120–27126, https://doi.org/10.1021/acsami.7b05634.
[38] A.K. Maity, J.Y. Lee, A. Sen, H.S. Maiti, Negative differential resistance in ferroelectric Lead zirconate titanate thin films: influence of Interband Tunneling on leakage current, Jpn. J. Appl. Phys. 43 (2004) 7155, https://doi.org/10.1143/JJAP.43.7155.
[39] D. Damjanovic, Ferroelectric, dielectric and piezoelectric properties of ferroelectric thin films and ceramics, Rep. Prog. Phys. 61 (1998) 1267, https://doi.org/10.1088/0034-4885/61/9/002.
[40] S.-J. Kim, S. Seelecke, A rate-dependent three-dimensional free energy model for ferroelectric single crystals, Int. J. Solids Struct. 44 (2007) 1196–1209, https://doi.org/10.1016/j.ijsolstr.2006.06.007.
[41] L. Pintilie, C. Ghica, C.M. Teodorescu, I. Pintilie, C. Chirila, I. Pasuk, L. Trupina, L. Hrib, A.G. Boni, N. Georgiana Apostol, Polarization induced self-doping in epitaxial Pb (Zr0. 20Ti0. 80) O3 thin films, Sci. Rep. 5 (2015) 14974.
[42] T.K. Song, Landau-Khalatnikov simulations for the ferroelectric switching in ferroelectric random access memory application, J. Korean Phys. Soc. 46 (2005) 5–9.
[43] M.S. Richman, P. Rulis, A.N. Caruso, Ferroelectric system dynamics simulated by a second-order Landau model, J. Appl. Phys. 122 (2017) 094101, https://doi.org/10.1063/1.5000139.
[44] J.F. Scott, Switching of ferroelectrics without domains, Adv. Mater. 22 (2010) 5315–5317, https://doi.org/10.1002/adma.201003264.
[45] G. Rosenman, D. Shur, Ya.E. Krasik, A. Dunaevsky, Electron emission from ferroelectrics, J. Appl. Phys. 88 (2000) 6109–6161, https://doi.org/10.1063/1.1319378.